A COMMON ERROR IN THE DETERMINATION OF AC PRIMARY TRANSFORMER CURRENT WAVEFORMS IN ONE-WAY HALF-WAVE RECTIFIERS

Edward Alexander Colin Lourenço*°, Wilson Komatsu*, Lourenço Matakas Jr.*°#, Walter Kaiser*
* Universidade de São Paulo (USP), ° Universidade São Judas Tadeu (USJT), # Pontifícia Universidade Católica (PUC-SP)

Escola Politécnica da USP - Av. Prof. Luciano Gualberto, trav. 3, no. 158 – 05508 900 São Paulo SP BRAZIL
wilsonk@usp.br

***Abstract* – The primary current of transformers feeding one-way half-wave rectifiers has some peculiarities that are often erroneously presented in Power Electronics textbooks. This paper explains some physical phenomena involved and proposes a simple mathematical model to reproduce the experimental current waveform by software simulation.**

***Keywords* – education, half-wave, one-way, rectifier, transformer magnetizing current.**

I. INTRODUCTION

Interesting discussions result when the authors propose to their students this basic question: "Which one of the waveforms shown in fig. 2 better describes the primary current i_1 in fig. 1 where a transformer feeds a single-phase half-wave rectifier?

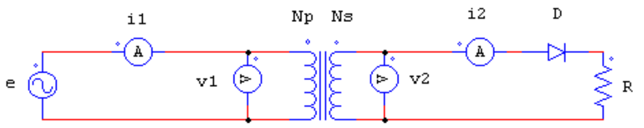

Fig. 1. Schematic diagram of a single phase, one-way, half-wave rectifier.

Answer (a) is very common, since it is quite similar to the waveform found in some Power Electronics textbooks [4, 5, 6, 7, 13]. By applying Ampère's and Faraday's laws, others could reason it should be answer (d), since in the ideal transformer, the total magnetomotive force is zero. Some students cannot answer, because this circuit is not presented in some textbooks [2, 3, 8, 9, 10, 11, 12, 14]. However, measuring this current in a laboratory, answer (e) should be evident but not intuitive.

Although the circuit is quite simple, it requires a thorough analysis and modelling. In 1962 Bertele and Grasl [1] proposed a qualitative analysis. In spite of its high technical value their paper did not receive the attention it deserved.

The contribution of this paper is to give a theoretical basis to justify the correct answer, presenting experimental measurements and simulations. Limitations of transformer models commonly adopted to explain the behaviour of half-wave rectifiers are also discussed.

The paper is organized as follows. Section II shows the relative influence of each transformer equivalent circuit parameter on the primary current wave shape in a single-phase half-wave rectifier. Section III presents experimental and simulated waveforms for single-phase and three phase half-wave rectifiers. Finally, conclusions are shown in section IV.

II. TRANSFORMER MODEL

The well-known transformer equivalent circuit [15] improved to better describe core saturation fully explains the operation of the single-phase half wave rectifier. To observe the influence of each circuit parameter on the primary current wave shape, the circuit of fig.1 is simulated by software (PSIM Demo v. 6.0 [16]). Beginning with the concept of ideal transformer the equivalent circuit model is improved by gradually adding all necessary elements until the behaviour of the simulated primary current is acceptable compared to the experimental waveform.

A. Ideal transformer

The ideal transformer shown in fig. 3a consists of two magnetically coupled coils having N_p and N_s turns and exhibiting the following properties:

a) perfect magnetic coupling between both windings;
b) neither winding nor core losses;
c) core magnetic material is linear with $\mu \rightarrow \infty$.

The relationship between an arbitrary primary voltage $v_p(t)$ and the core flux $\phi(t)$ is given by Faraday's law:

$$v_p(t) = N_p \frac{d\phi}{dt} \tag{1}$$

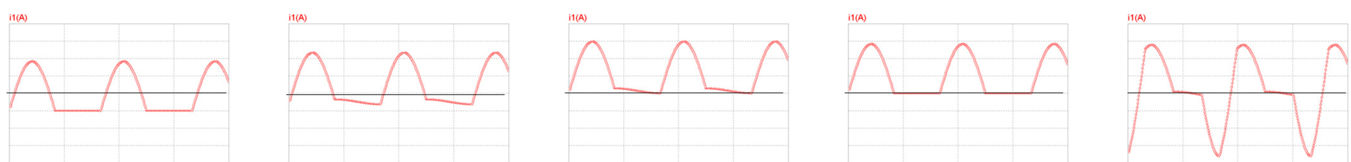

(a) (b) (c) (d) (e)

Fig. 2. Possible transformer primary current (i_1) waveforms of a single phase, one-way half-wave rectifier.

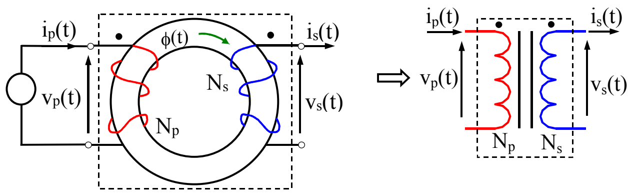

(a) Electric circuit. (b) Equivalent model.

Fig. 3. Ideal transformer.

The magnetic flux $\phi(t)$ linking both windings is given by:

$$\phi(t) = \frac{1}{N_p}\int_{t_0}^{t} v_p(\xi)d\xi + \phi(t_0) \tag{2}$$

For example, if the primary voltage $v_p(t)$ is sinusoidal, the core flux is sinusoidal with an average value which depends on the turn on instant t_0 as shown on (2).

Since coupling between windings is perfect (property a), the secondary voltage $v_s(t)$ is obtained from:

$$v_s(t) = N_s \cdot \frac{d\phi}{dt} = \frac{N_s}{N_p} \cdot v_p(t) \tag{3}$$

Note that (3) is valid for any primary voltage waveform, including DC voltages.

If the area of the core cross section is S, the magnetic flux density $B(t)$ results:

$$B(t) = \frac{\phi(t)}{S} \tag{4}$$

Assuming $i_s(t)$ null, $i_p(t)$ is obtained by applying Ampère's law to the magnetic field intensity $H(t)$ through a path of length ℓ:

$$i_p(t) = \frac{H(t).\ell}{N_p} \tag{5}$$

Since:

$$H(t) = \frac{B(t)}{\mu} \tag{6}$$

and assuming core material to be linear and without losses (properties b and c), when $\mu \to \infty$ (property c) the BxH curve becomes a vertical line at $H=0$. As a consequence, $i_p(t)$ is null for $i_s(t)=0$ and any finite change on B does not affect the null value of $i_p(t)$.

When a load current $i_s(t)$ flows in the secondary winding, according to Ampère's law, the total magnetomotive force must be null because $H=0$. Thus, the primary current can be calculated by:

$$i_p(t) = \frac{N_s}{N_p} \cdot i_s(t) \tag{7}$$

Note that (7) is valid for any secondary current waveform, including DC currents.

Note further that the voltages, given only by Faraday's law, and currents, given only by Ampère's law, are decoupled in an ideal transformer.

From (3) and (7), one gets:

$$v_p(t).i_p(t) = v_s(t) \cdot i_s(t) \Rightarrow p_p(t) = p_s(t) \tag{8}$$

showing that instantaneous primary and secondary power are equal, since this model neither stores nor dissipates energy.

Therefore, the electric behaviour of the ideal transformer can be represented by the equivalent electric circuit depicted in fig. 3b and by relations (3) and (7). These relations do not depend on frequency or waveform and both are valid for DC voltages and currents, respectively.

The single-phase half wave rectifier with ideal transformer is simulated (fig. 4) using $N_p=N_s=1$ [turns], $v_p(t)=e(t)=1.sin(\omega t)$ [volts], $\omega=1$ [rad/s], $R=1[\Omega]$. Notice that the ideal transformer available in PSIM Demo v. 6.0 [16] is the same as described in this section.

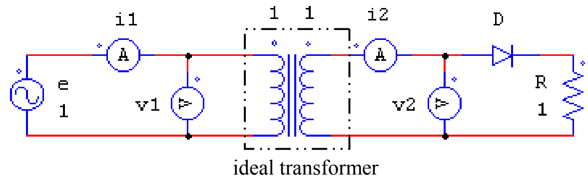

Fig. 4. Rectifier circuit with ideal transformer.

As expected, fig. 5a shows that currents i_1 ($=i_p$) and i_2 ($=i_s$) are coincident and fig. 5b shows that v_1 ($=v_p$) and v_2 ($=v_s$) voltages are equal.

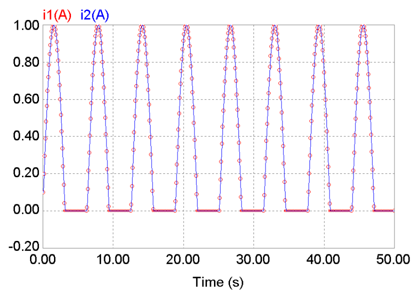

(a) Currents i_1 and i_2.

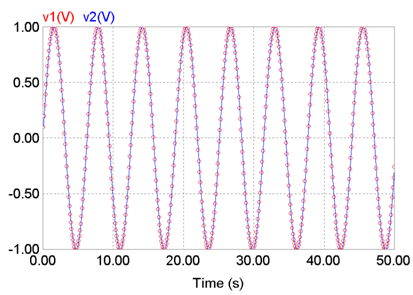

(b) Voltages v_1 and v_2.

Fig. 5. Simulated waveforms for rectifier with ideal transformer model.

The current i_1 corresponds exactly to fig. 2d and must have an average value. Its waveform differs significantly from the experimental one (fig. 2e).

B. Lossless linear transformer model

This model (fig. 6) is identical to the ideal one except for considering a finite and constant value for permeability μ. Thus, even when $i_s(t)$ is null, a magnetizing current (i_{mag}) must flow on the primary side of the transformer. Its value is derived from Ampère's law and calculated similarly to (5):

$$i_{mag}(t) = i_1(t) = \frac{H(t).\ell}{N_p} = \frac{B(t).\ell}{\mu.N_p} = \frac{\phi(t).\ell}{S.\mu.N_p} \tag{9}$$

Hence, the magnetizing current is proportional to the core flux, given by (2) and, if $v_p(t)$ is sinusoidal, $\phi(t)$ and $v_s(t)$ waveforms are also sinusoidal with average values that depend on the turn on instant t_0.

From (1) and (9):

$$v_p(t) = N_p \frac{d\phi}{dt} = \frac{N_p^2.\mu.S}{\ell} \frac{di_{mag}(t)}{dt} = L_{mag}.\frac{di_{mag}(t)}{dt} \tag{10}$$

The current i_{mag} has an inductive characteristic and is represented in the equivalent electrical circuit by the inclusion of an inductance L_{mag} on the ideal transformer model.

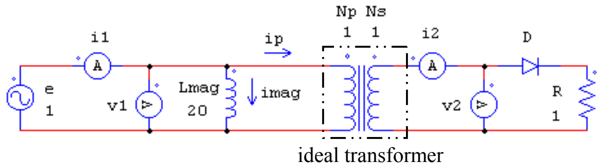

Fig. 6. Rectifier circuit with lossless linear transformer.

Notice that the primary (i_p) and secondary (i_s=i_2) winding currents must be equal to the load current when the turns ratio is one, but not identical to the primary side current $i_1(t)$ which is the sum of magnetizing current $i_{mag}(t)$ and primary winding current $i_p(t)$ for this transformer model (fig. 6).

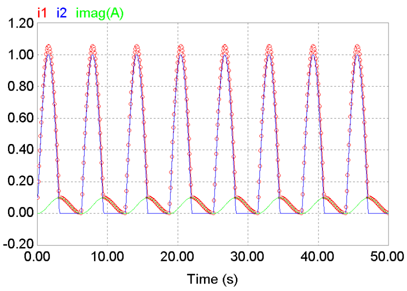

Fig. 7. Simulated current waveforms for rectifier with linear transformer model.

Primary current $i_1(t)$ on fig. 7 corresponds exactly to fig. 2c and <u>must</u> have an average value depending on the chosen initial conditions and parameters. Its waveform differs significantly from the experimental one (fig. 2e).

C. Linear transformer model with leakage inductances

The imperfect magnetic coupling between primary and secondary windings is represented in the electrical transformer model by inserting inductances in series with the windings [15] (fig. 8).

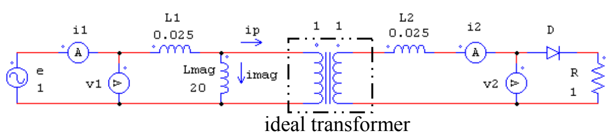

Fig. 8. Rectifier circuit with linear transformer with inductances.

One can see in fig. 9 that the inclusion of winding leakage inductances to the linear transformer model does not improve agreement with experimental primary current (fig. 2e).

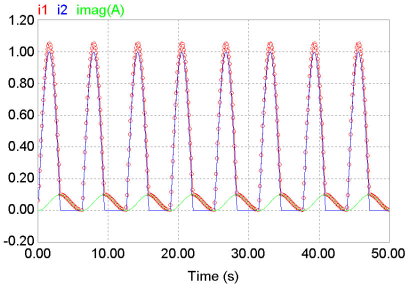

Fig. 9. Simulated current waveforms for rectifier with linear transformer model with leakage inductances.

Primary current $i_1(t)$ corresponds to fig. 2c and <u>must</u> have an average value. Its waveform differs significantly from the experimental one (fig. 2e).

D. Linear transformer with copper losses (only R_1) model

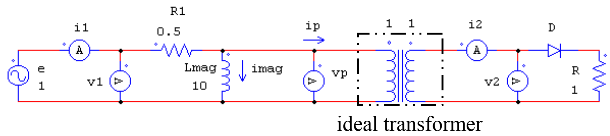

Fig. 10. Rectifier circuit with linear transformer and R_1.

Primary winding resistance R_1 is added to the linear transformer model. The secondary winding resistance can be considered incorporated to the load resistance.

Considering the circuit in fig. 10, its turn on with $e(t_0)=0$ and null initial conditions, one can see voltage drops on R_1 due to the reflected load current i_2 only in positive semi-cycles (figs. 11b and 11d). Voltage drops due to i_{mag} appear on negative and positive semi-cycles. Since the core flux is proportional to the integral of the primary winding voltage (2), this asymmetry on voltage drops on R_1 will drive the core flux to a negative average value, and, consequently, the magnetizing current will also have a negative average value.

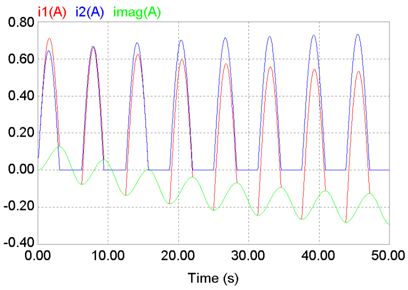

(a) Currents i_1, i_2 and i_{mag} in transient state.

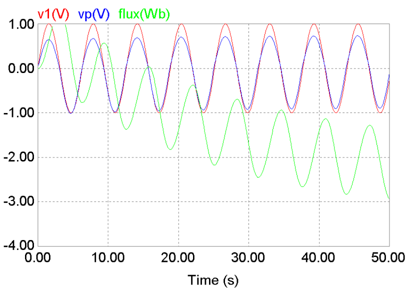

(b) Voltages v_1, v_p and linked flux in transient state.

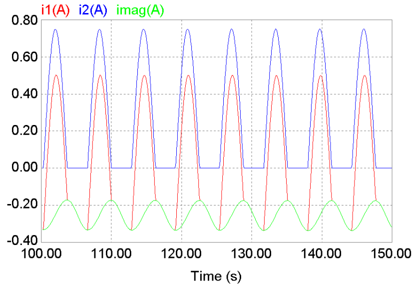

(c) Currents i_1, i_2 and i_{mag} in steady state.

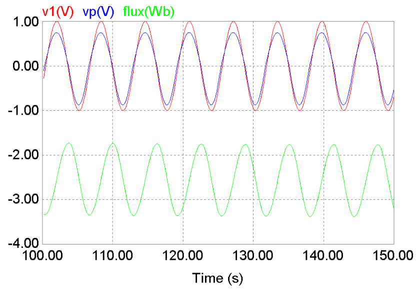

(d) Voltages v_1, v_p and linked flux in steady state.

Fig. 11. Simulated waveforms for rectifier with linear transformer with copper loss (only R_1) model

Primary current is the sum of primary winding current and magnetizing current. Thus, i_{mag} will decrease the negative peak value of the primary winding voltage until the average of this voltage becomes null, when the steady state is reached (fig. 11).

Primary current $i_1(t)$ corresponds exactly to fig. 2b and, on the contrary to the other cases, has a null average value, which does not depend on $e(t_0)$ value. Even though, $i_1(t)$ waveform differs significantly from the experimental one in the negative semi-cycle (fig. 2e).

E. Saturable transformer with copper losses (only R_1) model

Primary winding resistance R_1 is added to the saturable transformer model. The secondary winding resistance can be incorporated to the load resistance (fig.12).

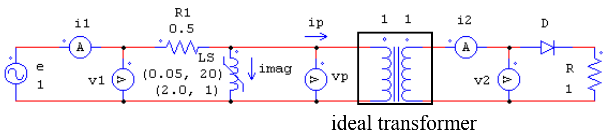

Fig. 12. Rectifier circuit with saturable transformer and copper losses.

The transient behaviour is similar to that of section II.D. Due to saturation of the transformer, the magnetizing current surpasses the saturation knee in part of the negative semi-cycle, resulting in considerable negative peak values in magnetizing and primary current waveforms. Consequently, the total transient time decreases when compared to the linear transformer case.

Primary current is the sum of primary winding current and magnetizing current (fig. 13). So, the negative peaks of i_{mag} will quickly decrease the negative peak value of the primary winding voltage $v_p(t)$ until its average value becomes null, when the steady state is reached.

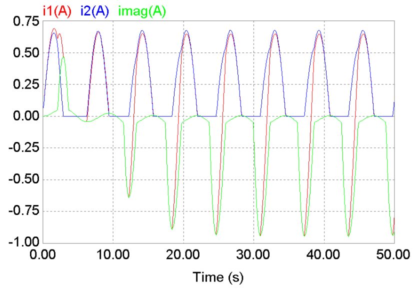

(a) Currents i_1, i_2 and i_{mag}.

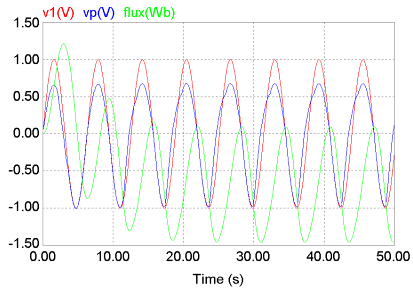

(b) Voltages v_1, v_p and linked flux.

Fig. 13. Simulated waveforms for rectifier with saturable transformer model and copper losses.

Primary current $i_1(t)$ has a null average value and its waveform is very similar to the experimental one (fig. 2e).

F. Preliminary conclusions

Based on all previously simulated waveforms, the following preliminary conclusions can be inferred:

a) No model can explain the common thinking that the primary current is obtained by subtracting from the reflected secondary current its average value (as shown in fig. 2a). Many Power Electronics textbooks adopted all over the world give this wrong explanation [4, 5, 6, 7, 13] or omit it [2, 3, 8, 9, 10, 11, 12, 14].

b) When the secondary winding current is reflected to the primary winding of the ideal transformer, it maintains its positive average value. What really happens is that the presence of the series resistance R_1 forces a negative bias in the magnetizing current $i_{mag}(t)$, resulting in a primary current $i_1(t)$ with null average value, as can be seen in the waveforms of figs. 11c and 13a. In steady state, the average voltage on the magnetizing inductance must be zero. This condition is satisfied only if, considering $e(t)$ with null average value, the average voltage drop across R_1 is also null, which implies $i_1(t)$ with zero average value.

c) For real cases, R_1 always exists, resulting in a null average primary current $i_1(t)$ (for $e(t)$ with null average value).

d) Furthermore, the high value of the negative peak current in fig. 13a is due to the saturation of the transformer core. Even for high values of magnetizing inductance, the negative area of the magnetizing current must be equal to the positive one of the reflected load current, forcing the

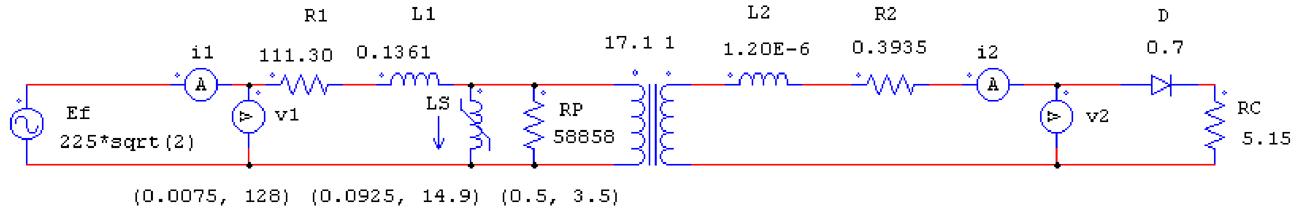

Fig. 14. Complete circuit model for single-phase simulations

with asymmetrical hysteresis loop, what causes a high degree of core saturation.

e) Notice that leakage inductances are not necessary to explain the circuit behaviour. The primary winding resistance and magnetic core saturation, commonly neglected in a first analysis, must be present in the transformer modelling in order to explain what happens in the real case.

III. EXPERIMENTAL AND SIMULATED RESULTS

A. Circuit model for simulations

The complete circuit model for single-phase simulations is shown in fig. 14. A saturable inductor L_s, available in the software PSIM Demo v. 6.0 [16], modelled by three straight lines, is applied in order to improve numerical results compared to the two lines saturation model of section II.E. Parameter values are in their corresponding units and were experimentally obtained (short-circuit and open-circuit tests) or adopted with usual values (e.g. the diode direct voltage drop). One must notice an open-circuit test must be performed with applied voltage values significantly higher than nominal ones in order to obtain the highly saturated magnetizing inductance.

For three-phase simulations, three single-phase transformers connected in delta-wye were applied, considering that the magnetization of each transformer does not affect the others. The three phase simulations were done on PSIM Full v. 5.0 [16] since the circuit exceeds the maximum number of components allowed in software PSIM Demo v. 6.0 [16].

B. Single-phase measurements

1) Steady state

Experimental and simulated waveforms are presented in fig. 15 for a single-phase rectifier with saturable transformer.

It can be seen that the experimental and simulated waveforms agree well.

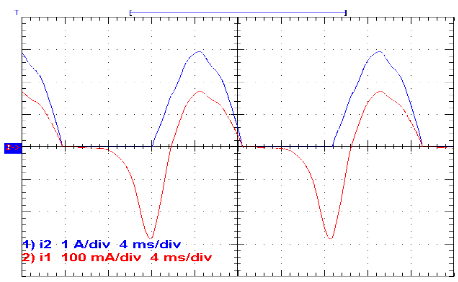

(a) Experimental primary and secondary current waveforms.

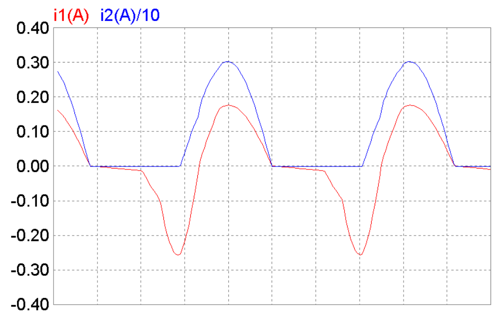

(b) Simulated primary and secondary current waveforms.

Fig. 15. Steady state primary and secondary current waveforms for a single-phase transformer.

2) Load insertion transient

Experimental and simulated waveforms for the primary current are presented in fig. 16 when a load is applied.

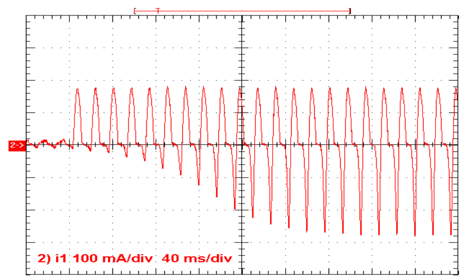

(a) Experimental primary current waveform.

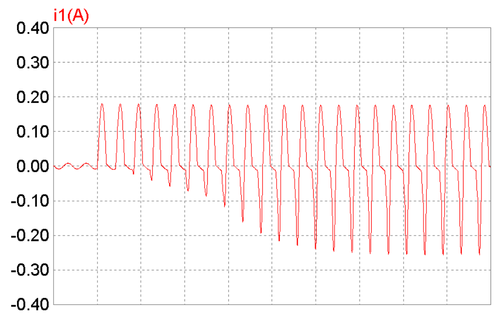

(b) Simulated primary current waveform.

Fig. 16. Load insertion transient primary current waveform for a single-phase transformer

It can be seen that the experimental and simulated waveforms agree well.

C. Active Power and RMS currents comparisons

Primary current rms value was calculated by two methods: a) Real case: from the measured waveform; b) Wrong model case: from the reflected load current waveform with its average value subtracted.

Active power was calculated by integrating the product of the instantaneous voltage and current values (real and wrong cases). Results are shown is table 1.

Table 1. Power and rms currents comparison

	Real primary	Wrong primary	Load
Voltage (rms) [V]	221	221	12,1
Current (rms) [mA]	121	60,3	14,4
Power [W]	15,1	12,3	12,0

By applying the wrong model, one underestimates the primary rms current and active power. The considerable difference between primary and load active powers is mainly from primary winding losses and it is neglected when using the wrong model.

D. Three phase measurements

Experimental waveforms and their corresponding simulated waveforms are presented in fig. 17 for a rectifier with a bank of three separated single-phase transformers.

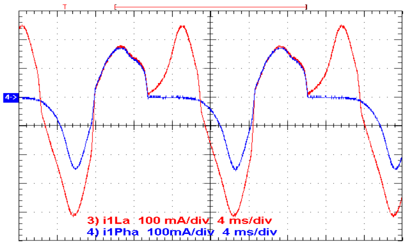

(a) Experimental phase and line primary current waveforms.

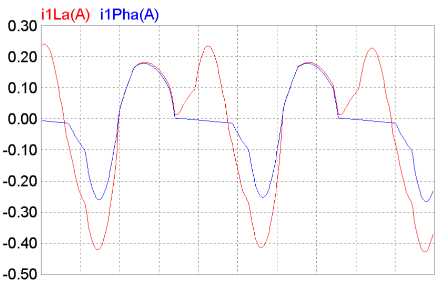

(b) Simulated phase and line primary current waveforms.

Fig. 17. Primary current waveforms for a three-phase, half-wave rectifier with a bank of three separated single-phase transformers.

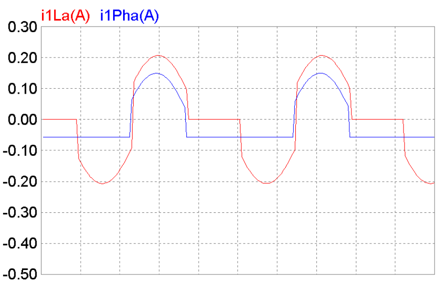

Fig. 18. Erroneous primary current waveforms for a three-phase, half-wave rectifier with a bank of three separated single-phase transformers.

It can be seen that the experimental and simulated waveforms agree well.

In fig 18 it is shown the erroneous primary line and phase current waveforms presented in some Power Electronics textbooks [4, 5, 7, 13]. It can be seen that these current waveforms differ significantly from the experimental and simulated ones (fig. 17).

IV. CONCLUSIONS

Experimental measurements show that the behaviour of single phase, one-way half-wave rectifier with transformer is erroneously presented and explained in many textbooks.

This paper has presented a step-by-step development of a simple model for a single phase, one-way half-wave rectifier with transformer, which adequately explains the real transformer behaviour. These results are also extended to a three phase one-way half-wave rectifier with a bank of single-phase transformers, validated by both experimental and simulated results.

There are two main results. The first one establishes that the transformer primary winding resistance plays an important role to explain the presence of the negative portion of the primary current, and its resulting null average value. The second one states that the core saturation, represented in the transformer model by a non-linear inductance, explains the high amplitude distorted waveforms.

It has been shown that a very simple transformer electrical model can perfectly explain the supposedly strange behaviour of the real waveform measurements on one-way half wave rectifiers. Although the limited practical utilization of this rectifier, it is useful to reinforce basic concepts of electromagnetism and electrical circuits.

REFERENCES

[1] Bertele, H von; Grasl, H. Anomalies in Converter Transformer Operation. Direct Current, London, p. 203-214. Aug. 1962;

[2] Mohan, N.; Undeland, T.M.; Robbins, W.P. Power Electronics: Converters, Applications and Design. New York, John Wiley & Sons, Inc. 2003, 3rd Edition;

[3] Rashid, M.H.; Power Electronics: Circuits, Devices and Applications. New Jersey, Prentice Hall, 1993, 2nd Edition;

[4] Möltgen, G. Line Commutated Thyristor Converters. Siemens Aktiengesellschaft and Pitman Publishing, Berlin-Munich, London. 1972.

[5] Schaefer, J. Rectifier Circuits: Theory and Design. John Wiley and Sons, New York, 1965.

[6] Kimbark, E.W. Direct Current Transmission. Wiley-Interscience, New York, 1971, v.1;

[7] Barton, T.H. Rectifiers Cycloconverters and AC Controllers. Clarendon Press, Oxford, 1994.

[8] Paice, D.A. Power Electronics Converter Harmonics: Multipulse Methods for Clean Power. IEEE Press, Piscataway, 1996.

[9] Thorborg, K. Power Electronics. Prentice Hall, New York, 1988.

[10] Bird, B.M.; King, K.G.; Pedder, D.A.G. An Introduction on Power Electronics. John Wiley & Sons, Chichester, 1993, 2nd Edition.

[11] Hart, D.W. Introduction to Power Electronics. Prentice Hall, Upper Saddle River, 1997.

[12] Erickson, R.W. Fundamentals of Power Electronics. Chapman & Hall, New York, 1997.

[13] Barbi, I. Eletrônica de Potência. Edição do Autor, Florianópolis, 2000. 3rd Edition (in Portuguese)

[14] Batarseh, I. Power Electronics Circuits. John Wiley & Sons, New York, 2004.

[15] Massachusetts Institute of Technology (MIT) Staff. Magnetic Circuits and Transformers. John Wiley & Sons, New York, 1943.

[16] Powersim Inc. PSIM User's Guide. Powersim Inc., Andover. Available in http://www.powersimtech.com . Site accessed in January 1st, 2005.